Scientific Research Publishing

World Journal of Engineering and Technology, 2024, 12, 742-758
https://www.scirp.org/journal/wjet
ISSN Online: 2331-4249
ISSN Print: 2331-4222

Metallurgical Forensics: Investigating a Superheater Tube Failure in Industrial Process Plants

Kok Toong Leong

Engineering Department, QSM Associates, Singapore
Email: leong.kt.qsm@gmail.com, leongkt@qsmassociates.com.sg

How to cite this paper: Leong, K.T. (2024) Metallurgical Forensics: Investigating a Superheater Tube Failure in Industrial Process Plants. *World Journal of Engineering and Technology*, **12**, 742-758.
https://doi.org/10.4236/wjet.2024.123046

Received: July 13, 2024
Accepted: August 18, 2024
Published: August 21, 2024

Abstract

A metallurgical forensic investigation was conducted to determine the cause of a failed superheater tube. Analysis techniques by Visual Examination, Energy Dispersive X-ray Analysis, Mechanical Testing and Metallographic Investigation were conducted, together with a comparative study from an inlet elbow section that did not fail. The superheater tube suffered premature failure after being in service for about two years. It was concluded that the failed tube underwent overheating, corrosion-erosion, embrittlement, and eventual failure under its internal pressure by stress rupture. The analysis revealed intergranular cracks, window fracture features and spheroidization of pearlite with grain growth. A possible contribution to embrittlement was from copper. Follow-ups and recommendations were provided, as well as covering materials, inspection, and operational considerations.

Keywords

Superheater Tubes, Thermal Degradation, Corrosion-Erosion, Embrittlement, Stress Rupture

1. Introduction and Background

Boilers are an integral part of a process plant including petrochemical and power generation. A failure in the boiler's superheater can lead to a process plant shutdown, costing millions of dollars. Superheater tubes in a boiler elevate the temperature of steam, converting it from saturated to superheated steam. Saturated steam exists at its boiling point for a given pressure, while superheated steam is heated beyond this point.

The primary function of a superheater is to utilize the heat from combustion gases to increase the steam's temperature, thereby improving the efficiency and

performance of steam turbines. However, the harsh operating environment subjects these tubes to various failure mechanisms. Some known superheater tube failures include:

• Creep rupture: This occurs due to prolonged exposure to high temperatures and stresses, leading to the gradual deformation and eventual failure of the material. An estimated 10% - 30% of boiler tube failures are caused by this mechanism [1].

• Thermal & Corrosion fatigue: This results from cyclic thermal stresses due to frequent temperature fluctuations. At times, corrosion becomes a factor, resulting in both corrosion and thermal mechanisms working together with fatigue. Thermal fatigue and corrosion fatigue are among the top 10 causes of failure in boiler industries [2].

• Erosion: This is when high-velocity steam and particulates wear away the tube's inner surfaces. Tube failures by erosion in some situations can account for a third of tube failures and can be as fast as 16,000 hours in service [3].

• High Temperature Corrosion occurs due to aggressive species like sulphur, alkaline salts, oil ash, coal ash and scaling as well. Much research focuses on temperature resistance but a combination has been a challenge [4].

Information regarding the failed superheater tube was provided. The failed superheater tube in this investigation failed unexpectedly in about just two years of operations. It was a parallel flow superheater. After the failure, the superheater continued to be used for another three weeks. The conditions under which the tubes operated were:

• Tube internal transported steam at about 350˚C with a pressure of 300 psi (See **Table 1** for boiler water analysis)

Table 1. Boiler water analysis.

Description	Water Sample 1	Water Sample 2
Conductivity	1.1 mS/cm	1.3 mS/cm
pH	9.64	10.0
P-Alkalinity	<0.1 mg/l $CaCO_3$	<0.1 mg/l $CaCO_3$
Iron (sample + 30% HCl)	13.9 mg/l	20.2 mg/l
Phosphate	7.0 mg/l	6.0 mg/l
Silica	200 micrograms/l	200 micrograms/l
Na^+	232 micrograms/l	292 micrograms/l
Sulphide	0.62 mg/l	0.57 mg/l
TDS[#1]	0.52 g/l	0.62 g/l
TSS[#2]	25 mg/l	40 mg/l
Chloride	96.4 ppm	102 ppm
Remarks Iron in filter after digested with HCl	53.7 wt%	38 wt%

[#1]: Total Dissolved Solid, [#2]: Total Suspended Solid.

• Hot fuel gas of about 800˚C (see **Table 2** for fuel oil analysis)

• Tubes were made of DIN 17175 St35.8 material

Table 2. Fuel oil analysis.

Description	Analysed Value
U50	*42.82
Flash Point	286˚C (COC[#1])
Specific Gravity @ 15˚C	1.037
Process Point ˚C	45˚C
CCR[#2] wt%	25.7 wt% (MCRT[#3])
Water Content vol%	<0.05 vol%
Ash Content % (m/m)	0.04% (m/m)
Vanadium	29 mg/kg
Total N	2253 mg/kg
*VK @ 100˚C = 1239 CST	

[#1]: Cleveland Open Cup. [#2]: Conradson Carbon Residue. [#3]: Micro Carbon Residue Tester.

2. Experimental Procedure

2.1. Method of Investigation

The following metallurgical analysis techniques were employed to investigate the cause(s) of superheater tube failure.

1) Visual Examination

This was to visually examine the failed components with naked eye in detail to appraise the failure locations, the initiation point, and the necessary steps for further examination & analysis in order to reach the root cause of the failure. It enables the visualization of the failure and generates a roadmap for conducting this failure analysis.

2) Metallographic Investigation

This investigation studies the microstructure of the tubes at various decisive locations that will shed light on the failure mechanism(s) and material condition. Specimens will be prepared in accordance with ASTM specification [5] [6]. It dwells deep into the material condition and reveals critical evidence of the final failure.

3) Energy Dispersive X-Ray Analysis (EDX)

This spectroscopy analytical technique is used for chemical elemental analysis on the surface. While it does not provide quantitative data, it can estimate the relative abundance of elements in the analyzed location. It offers a qualitative indication of the material's elemental composition and any foreign elements on the surface, providing insights into material composition and any environmental influence and/or corrosion product on the analyzed area.

4) Mechanical Testing—Hardness

This test provides information on the hardness values and can be converted to the tensile strength of the tube material at the tested location. This will provide an understanding of the strength of material at the failed and operating region in comparison with the material specifications. Test was carried out in accordance with ASTM Specification [7].

2.2. Visual Examination

Two superheater tubes were inspected. The first tube was the failed tube with an opening, as shown in Figure 1. A layer of material had been lost in the failed zone near the ruptured surface. A closer inspection revealed corrosion on both the external and internal surfaces of the failed zone, as presented in Figure 2 and Figure 3. It was also observed that the edges of the opening were slightly thinner compared to other areas. Further analysis using other techniques will focus on the failed zone, particularly the thinned areas and edges.

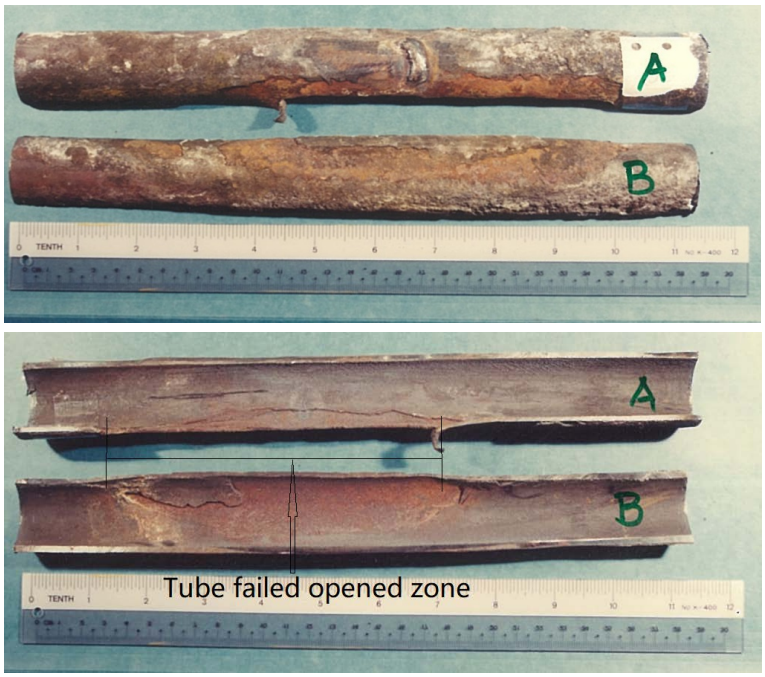

Figure 1. Picture of Failed Superheater Tube that was cut in half.

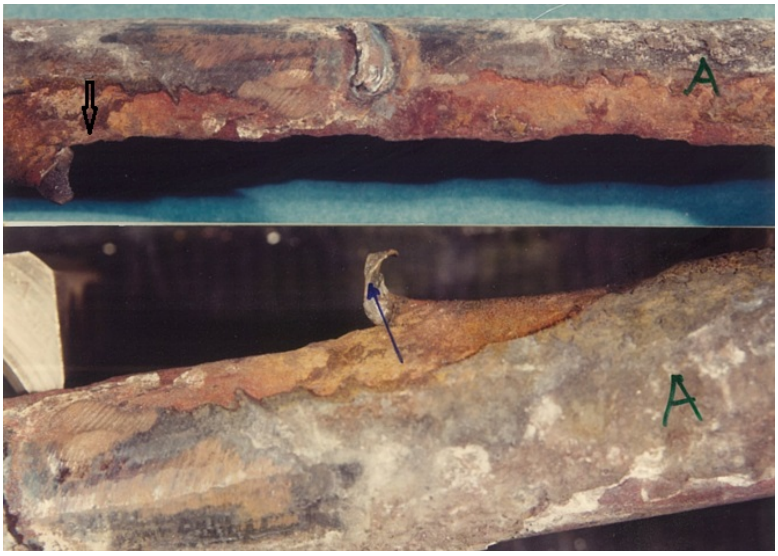

Figure 2. Corrosion seen on external surfaces (arrowed examples) of failed zone.

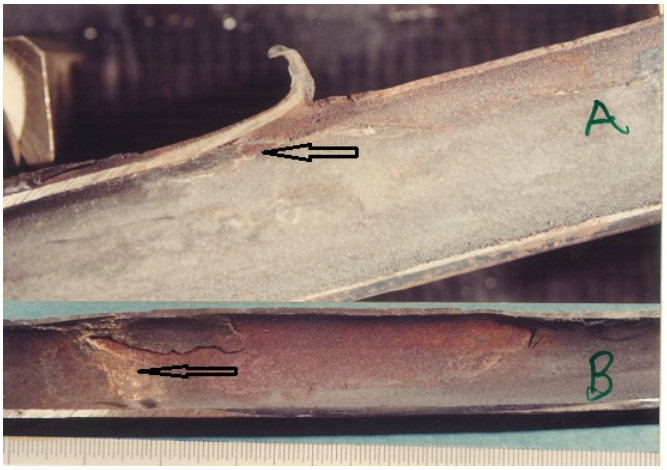

Figure 3. Corrosion seen on internal surfaces (arrowed examples) of failed zone.

In Figure 4, the rupture zone had a missing rectangular slice of tube material. This intriguing feature suggests a specific degradation mechanism that caused the section to be "torn off", and this rectangular section was not found on site.

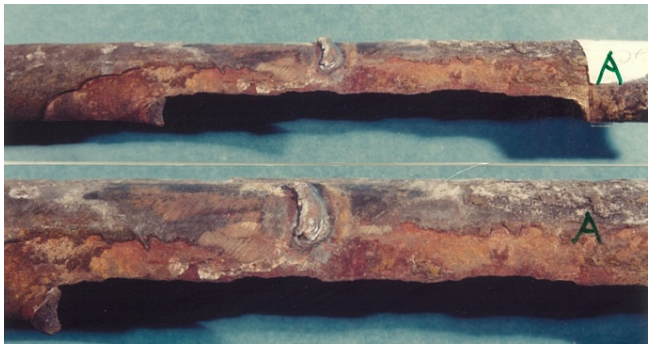

Figure 4. Failed opening exhibited a rectangular slice of the tube material that was lost. A window fracture appearance.

The second superheater tube was an elbow at the superheater inlet zone, away from the failed tube. Figure 5 shows this inlet elbow, where the external condition of the elbow did not show signs of corrosion or material loss. However, internal corrosion was clearly noted.

2.3. Metallographic Investigation

Two specimens from the failed tube were taken for metallographic Investigation. Specimens were taken at the fractured zone, in both longitudinal and transverse sections. The longitudinal section specimen preserved the fractured surface for longitudinal evaluation (marked E in Figure 6), while the transverse section cut across both semi-circular halves of the tube (marked A in Figure 6). The macro views of these two metallographic specimens are shown in Figure 6. For the purpose of comparative reference and study, a third specimen was studied by taking a cross-section from the superheater inlet elbow (marked D in Figure 6).

Figure 5. Superheater Inlet Elbow. Obvious corrosion products were seen on the internal surface (arrowed example).

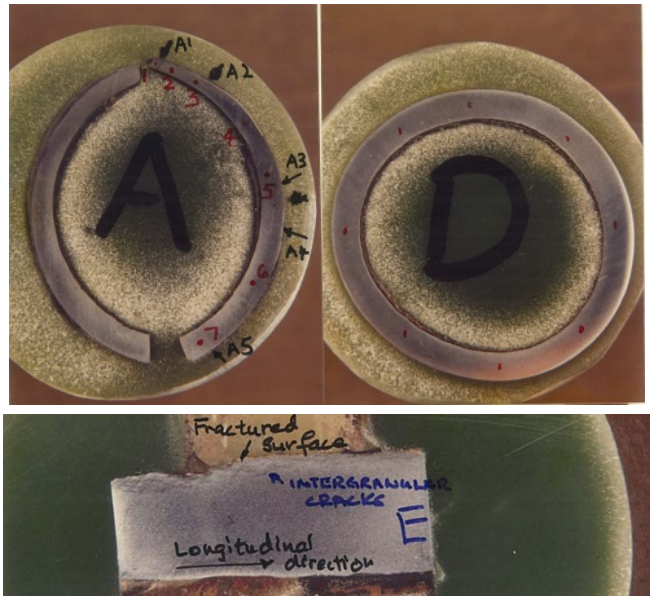

Figure 6. Macro view of Metallographic Specimens. A & E taken from failed tube and D from inlet elbow.

Fractured Superheater Tube Transverse Specimen A

It can be seen that A1 to A5 were marked on the transverse section. Location A1 was at the fracture surface zone. Moving along from locations A2 to A5, reaching the opposite of the fractured surface of the semi-circular section. A 20× macro view starting from A1 (the fracture opening) is shown in Figure 7. In this figure moving slightly away from the fracture zone, cracks can be seen to open from the external wall.

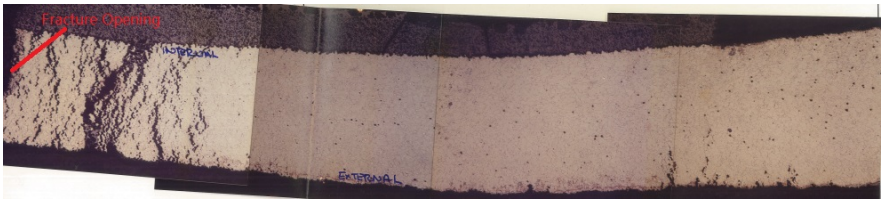

Figure 7. A 20× magnification of specimen A, starting from A1.

Figure 8, taken at 200× magnification, showed the microstructure at the A1 fractured surface. It displayed openings along a significant number of grain boundaries, indicating intergranular cracking. The microstructure reveals that the pearlite had undergone complete spheroidization forming spheroidized carbides with grain growth. This was a sign of severe thermal degradation.

Figure 9, taken at 200× magnification, showed the microstructure at the A2 location, a short distance from the fractured surface. This micrograph also revealed that the pearlite had undergone complete spheroidization forming spheroidized carbides with grain growth. However, the extent of intergranular cracks was much less, with smaller openings.

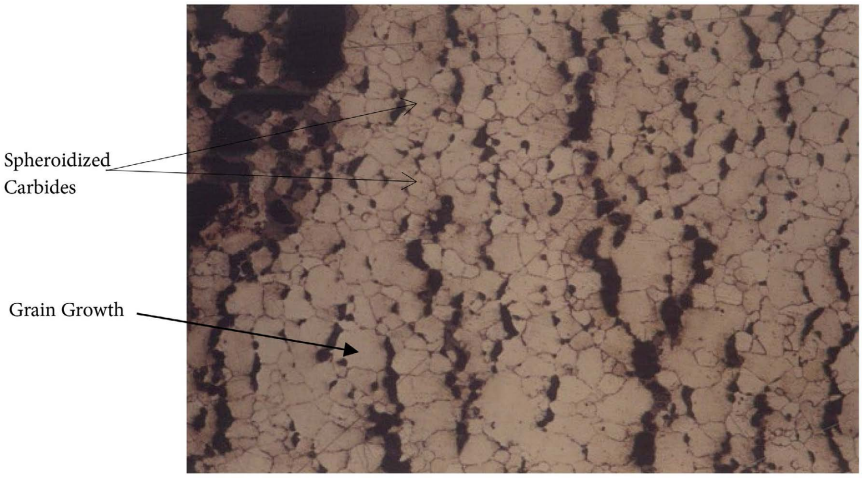

Figure 8. Micrograph of A1 at 200× magnification.

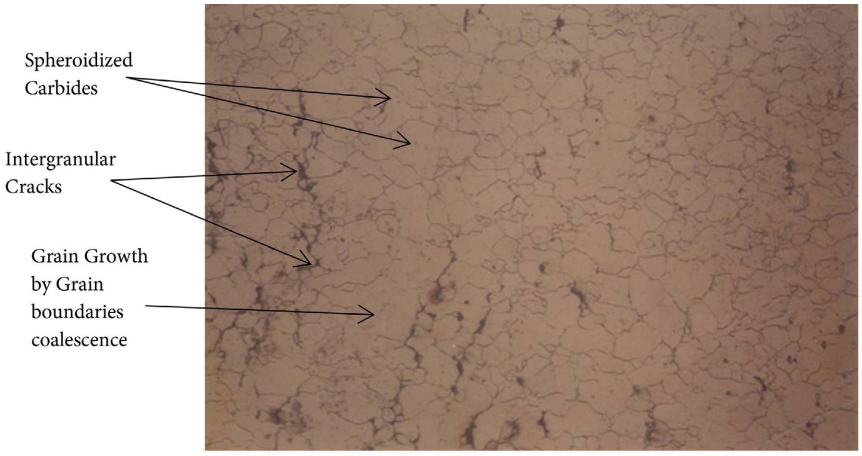

Figure 9. Micrograph of A2 at 200× magnification. No Pearlites were seen.

Figure 10, taken at 200× magnification, showed the microstructure at the A3 location, about a quarter of the circumference away from the fractured surface. This micrograph revealed the spheroidization of pearlite into spheroidized carbide accompanied by grain growth. Although grain growth was visible across the entire thickness of the material, it was more pronounced on the external wall compared to the internal wall.

Figure 10. Micrograph of A3 at 200× magnification.

Figure 11, taken at 200× magnification, showed the microstructure at the A4 location, more than a quarter of the circumference away from the fractured surface. This micrograph also revealed that the pearlite had undergone complete spheroidization into spheroidized carbides. Grain growth was evident in the external wall region but was not much in the internal region.

Figure 12, taken at 200× magnification, showed the microstructure at the A5 location, almost half the circumference away from the fractured surface. This micrograph revealed that the internal wall had a mixture of spheroidized carbides, pearlites and ferrite. Meanwhile, the external wall region had a mixture of spheroidized carbides, pearlite, ferrite and some grain growth. At the same magnification, the grains were obviously bigger on the external wall.

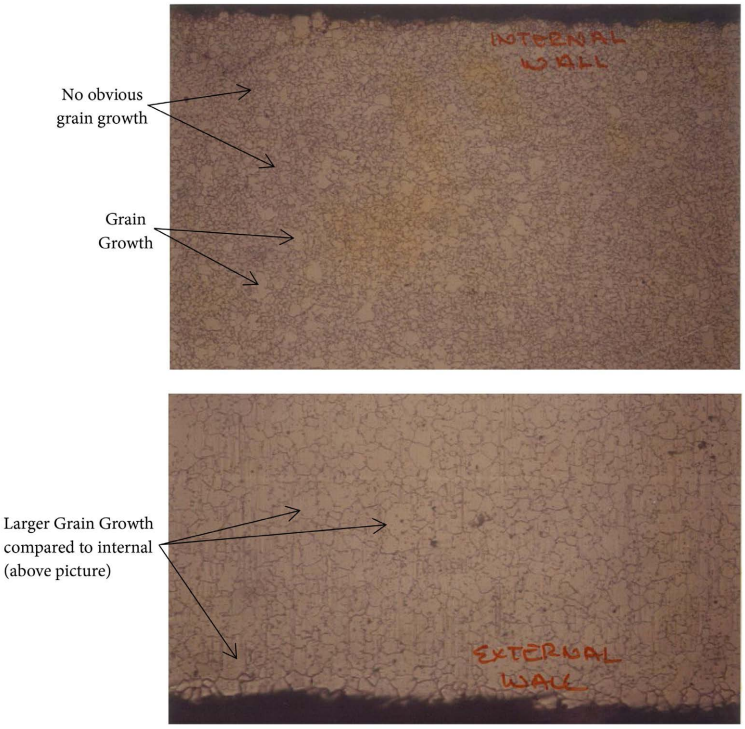

Figure 11. Micrograph of A4 at 200× magnification.

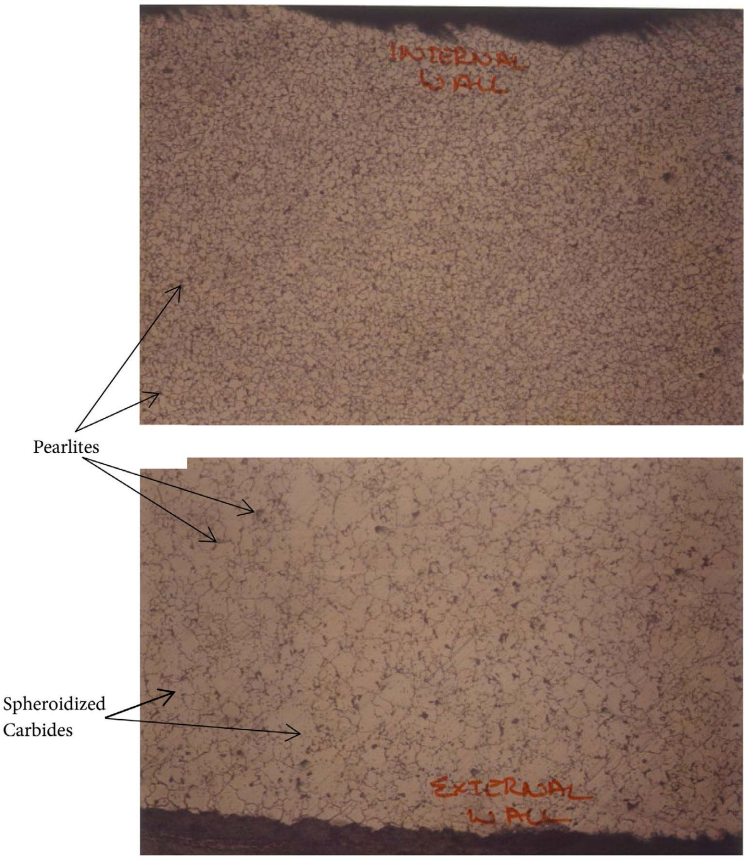

Figure 12. Micrograph of A5 at 200× magnification. Larger grain growth and greater spheroidization on external surface.

Fractured Superheater Tube Longitudinal Specimen E

Corresponding to longitudinal specimen E in Figure 6, the microstructure near the fractured surface was evaluated. Figure 13 below presents the observed condition. The pearlite had undergone complete spheroidization into carbides with significant intergranular cracking and tearing at the fracture surface region. Clearly the severity of the tearing from intergranular cracking was greater when it was closer to the fractured surface.

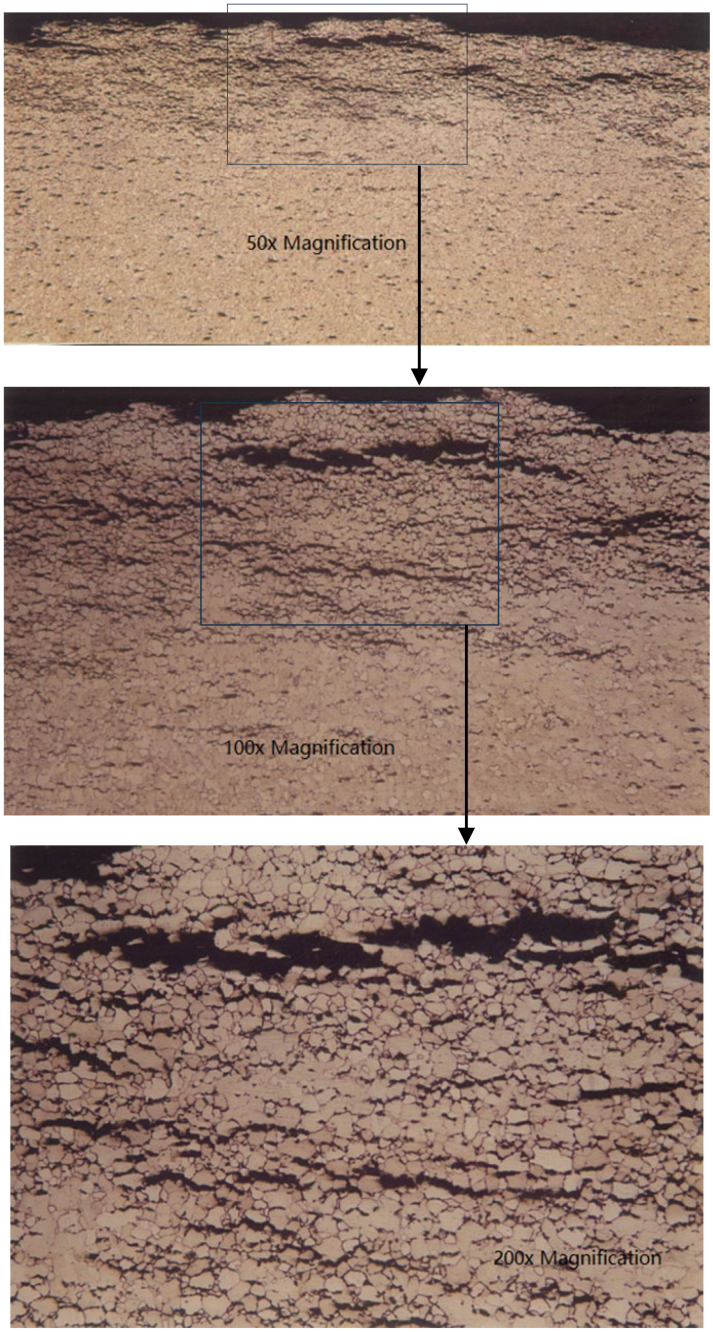

Figure 13. Micrograph of longitudinal specimen E, taken at fractures surface with 50×, 100× and 200× magnification.

Superheater Inlet Elbow Specimen D

The microstructure of the superheater inlet elbow was evaluated and was presented in Figure 14 below. This section shows a ferritic structure with pearlite and ferrite, exhibiting minor thermal degradation. This microstructure was consistent throughout the specimen.

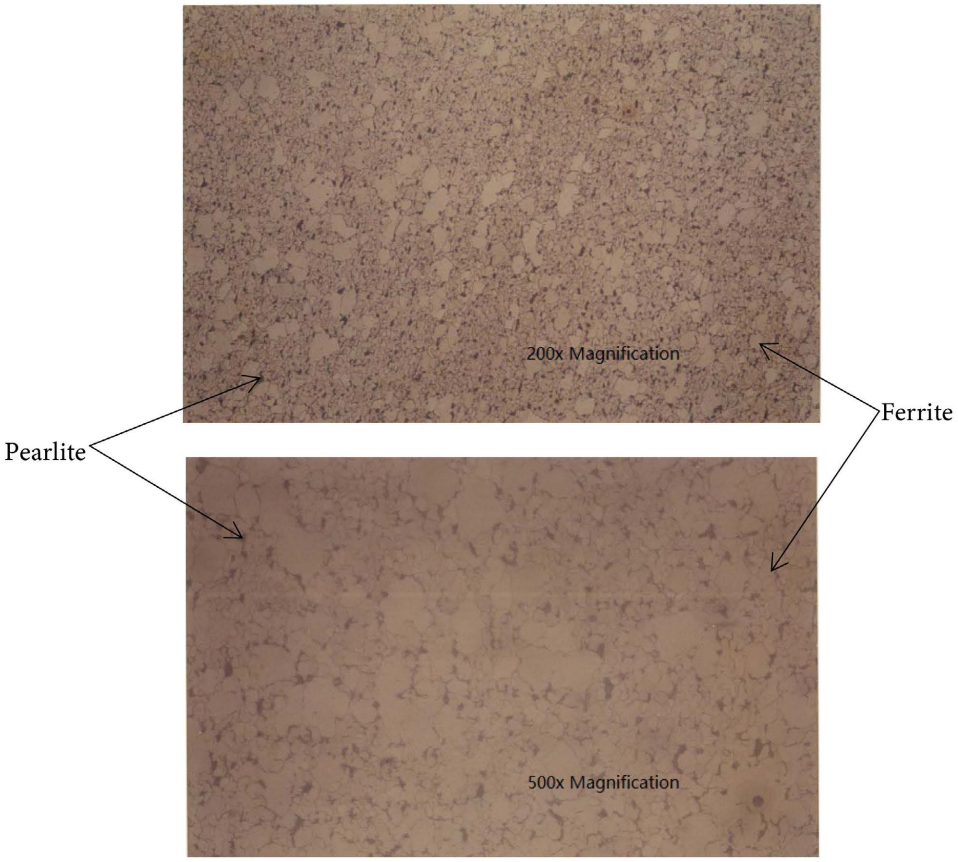

Figure 14. Micrograph of Superheater Inlet Elbow at 200× & 500× Magnification. Ferritic structure consisting of ferrite and pearlite can be seen.

2.4. Energy Dispersive X-Ray Analysis (EDX)

The chemical composition of the tube material, is as follows:

Energy Dispersive X-Ray Analysis was conducted on three areas to determine the elemental content of the corrosion products on the tubes.

The internal and external surfaces of the failed superheater tube were analyzed. Figure 15 & Figure 16 presents the resulting spectra of the EDX spectra. As seen in Figure 15, EDX detected the presence of aluminum, Sulphur, calcium, vanadium, manganese, iron, nickel, and copper on the internal of the failed superheater tube. On the external surface spectra in Figure 16, the presence of aluminum, sulphur, calcium, vanadium, manganese, iron, nickel, and copper. While the elements detected were the same, the proportions displayed were different. Sulphur and copper proportional ratio was bigger on the external surface as they were from the environment.

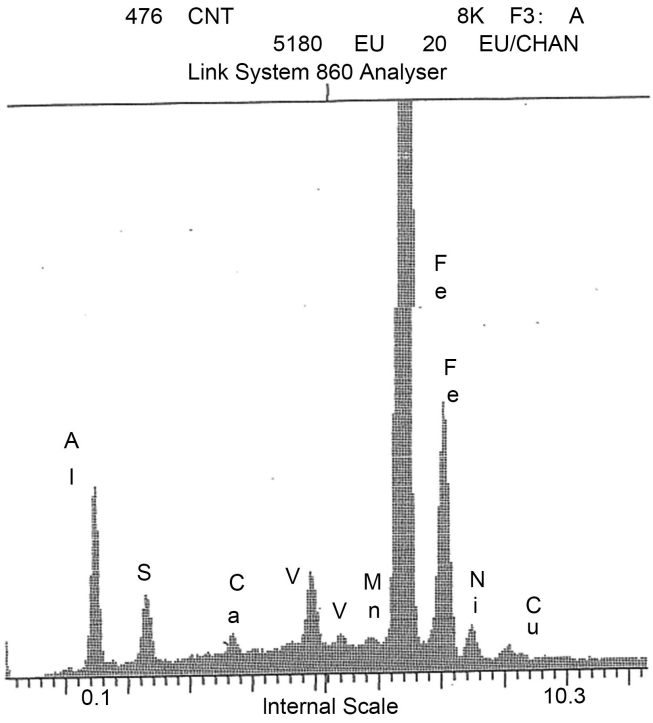

Figure 15. Ruptured Superheater Tube Internal Surface EDX Spectra.

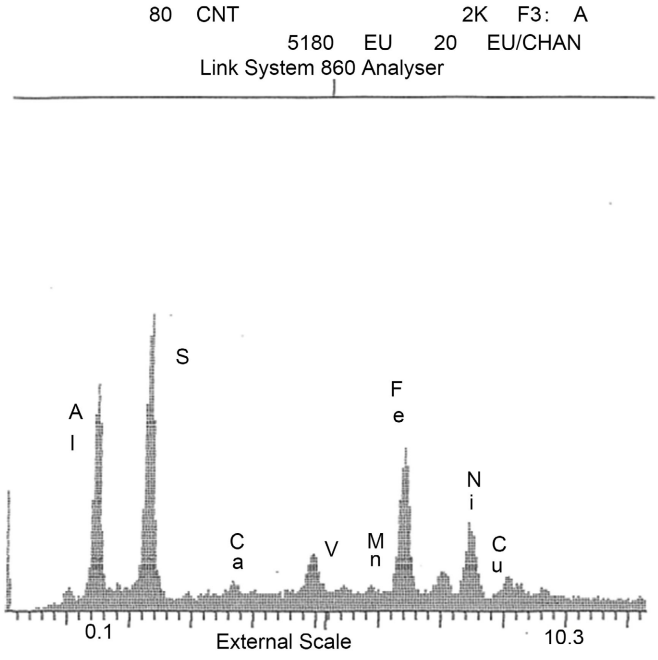

Figure 16. Ruptured Superheater Tube External Surface EDX Spectra.

EDX was also performed on the internal scale of the inlet elbow. Figure 17 presents the detected elements. EDX detected the presence of aluminum, silicon, sulphur, chloride, potassium, calcium, vanadium, manganese, iron and nickel. Most of these were elements from the based material (See Table 3) and others from the boiler water.

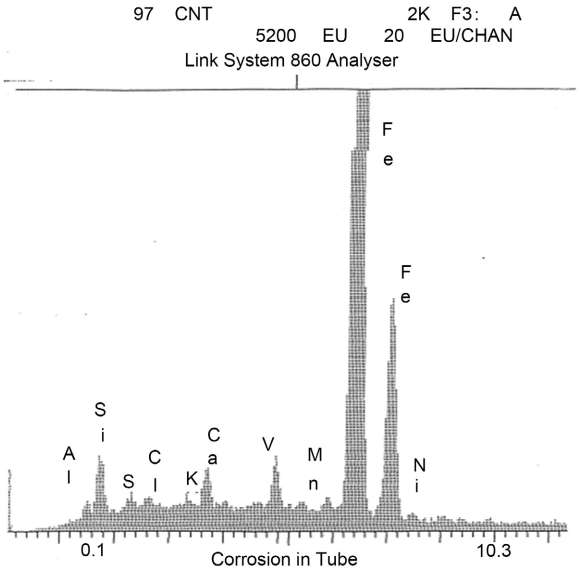

Figure 17. Superheater inlet elbow Internal Surface EDX Spectra.

Table 3. Chemical composition. [11]

DIN 17175	C	Si	Mn	P (max)	S (max)
St 35.8	≤0.17	0.1 - 0.35	0.4 - 0.8	0.04	0.04

2.5. Mechanical Testing—Hardness

The mechanical strength of the tube material is as follows in **Table 4**.

Hardness testing was conducted on failed superheater tube specimen A and inlet elbow specimen E. The data was tabulated in **Table 5**.

Table 4. Mechanical Properties @ Room Temperature [11].

DIN 17175	Tensile Strength (N/mm^2)	Minimum Yield Strength (N/mm^2)	Minimum Elongation Percentage	Minimum Impact Strength Joules
St 35.8	360 - 480	235	25	34

Table 5. Hardness testing results.

Locations[#1]		Results HV 5Kgf
Specimen A	1	102
	2	112
	3	114
	4	115[#2]
	5	120
	6	142
	7	147
Specimen D[#3]		155

[#1]: Refer to **Figure 6** for hardness locations, marked with red dots. [#2]: DIN 17175 Grade St35.8 minimum tensile strength = 360 MPa. Equivalent to 115HV. [#3]: Average value. The variations in reading were not significant.

3. Experimental Results Discussion & Analysis

The material quality of the superheater tubes was reportedly verified during the fabrication of the boiler. Therefore, further testing of this material quality was not carried out and it was assumed to have met the requirements of DIN 17175 St35.8 material.

3.1. Cracks Initiated from External and a Brittle Fracture

The cracks started from the outside, as evidence from **Figure 7** that cracks had developed along the external surfaces and they were not seen from the inside. The failed region had a relatively rectangular opening, with some material loss around this area (**Figure 4**). The rectangular like feature appeared typical of a window fracture [8] and is a known tube failure appearance associated with embrittlement. The intergranular crack, lack of shearing seen in the microstructure and no plastic deformation [9] supported features of a brittle fracture.

3.2. Thermal Degradation by Overheating

Metallographic Investigation revealed intergranular cracks in the failed region, particularly severe at the fracture opening. Additionally, thermal degradation was observed in this area, ranging from complete spheroidization of pearlite into spheroidized carbide, with grain growth at the fracture surface to partial spheroidization on the opposite circumference end of the tube's cross section.

When a plain carbon steel is overheated over a period of time, spheroidization takes place. Spheroidization is a change in the microstructure of steels around 440˚C to 760˚C range, where the cementite (Fe_3C) in the pearlite of carbon steels becomes unstable, dissolute and transforms from their normal plate-like form to small finely dispersed round spheroidized carbides form [10]. As spheroidization continues, grain growth will start to occur. The spheroidization and grain growth process softens the material causing it to loss in the material's strength.

The variation in microstructure across the cross section of the tube pointed towards differing temperatures along the circumference of the tube, with the failed zone anticipated to have been subjected to direct impact by the fuel gas. Consequently, the degradation and hence the material strength varied around the tube's circumference, as indicated by the hardness testing results shown in **Table 5**. This steel's minimum tensile strength 360 MPa [11] corresponds to a 115 HV hardness [12]. The hardness and thus strength in the vicinity of the fractured region was notably lower, falling well below that of DIN 17175 St35.8 material, while the region opposite showed the highest hardness, well within the strength of this material.

The superheater tube was made of DIN 17175 St35.8 material, designed for use up to 600˚C [11]. Application at temperatures above 600˚C and below austenitic temperature (around 727˚C) will accelerate thermal degradation and shorten the expected lifespan of this steel. Evidence existed in this failed super-

heater tube and there were signs of degradation in the inlet elbow as well, an indication of operating temperature beyond the design limits. In short, overheating and biggest contributor to the failure. The failed region is believed to be greater than 600˚C.

3.3. Corrosion-Erosion

Thinning was also observed at the fractured region, together with corrosion products being present, it signals a corrosion-erosion effect. A layer of thin corrosion products was observed on the internal and external walls of the failed tube. EDX spectra showed the presence of similar elements (refer to **Figure 15** and **Figure 16**). The detection of aluminum was likely due to contamination from the specimen holder. Elements such as sulphur and copper were likely derived from fuel oil gases and the surrounding environment. Comparing the information between the submitted fuel gas and boiler water analysis, EDX spectra of the failed tube and inlet elbow, it is deduced that the corrosion product layer inside the failed tube was formed after the tube had failed. Being a localized failure on one side of the tube, it is anticipated that a flow of gas must have been directed on that surface. This flow of gas created an erosive effect and the sulphur had a corrosive effect in that region. Thinning is, therefore, a result of corrosive-erosion effect, and a secondary contributor.

3.4. Embrittlement

Brittle fracture for plain carbon steel usually occurs at low temperature unless there are other mechanism present. However, this failure exhibits features of brittle fracture and window fracture feature points toward embrittlement [12]. One well known embrittlement mechanism in boiler tubes is hydrogen. However, for this case, the visual examination and metallographic investigation did not reveal any signs of decarburization, thick deposits, or hydrogen migration, thereby ruling out hydrogen embrittlement [8].

High sulphur proportion and copper existed in both the inside and outside of the failed tube and not in the inlet elbow. The EDX spectra for the inlet elbow corrosion product was consistent with the boiler water analysis and the tube material and did not show copper being present. Copper was also not part of the chemical composition of this grade of steel [11].

With all the evidences found, molten copper was the only source of liquid metal embrittlement and at temperature of about 480˚C was sufficient for liquid embrittlement by copper to occur [13], the smallest contributor in this failure.

3.5. Creep Rupture & Stress Rupture

While thermal degradation and spheroidization are not contestable in this failure, the failure lacks indications of creep rupture as evidence of typical creep rupture includes thinning and deformation from loss of strength and with creep cavities and voids forming along grain boundaries [14]. Intergranular cracks

started from an external surface and beyond the intergranular cracks zone, no other signs of grain boundary sliding or creep cavities at grain boundaries were found. Therefore, while the estimated temperature of the tube fits a 0.4 Tm [9] creep rupture was not concluded. This failure fits better into high temperature stress rupture in a localized zone which has some features of creep rupture. A feature of a purely typical high temperature stress rupture would be a fish-mouth feature, bulging or flattening [15]. However, this facture surface has a window fracture feature, indicating more than localized overheating high temperature stress rupture.

3.6. Lost Evidence

Valuable evidences were lost because the tube was used continuously for three weeks after the failure, making the exact state of the internal wall and the fractography of the first fractured surface unknown.

4. Conclusion

Based on the discussion, it is inferred that direct exposure of the failed region to fuel oil gases caused mainly thermal degradation from overheating, material thinning from corrosion-erosion, and possible embrittlement (potentially from molten copper) in the failed section of the superheater tube. The internal steam pressure in the tube eventually led to stress rupture. While molten copper embrittlement is a possible cause, other factors cannot be dismissed due to the tube's continued use for three weeks, resulting in the loss of vital evidence.

5. Follow-Ups and Recommendations

It is recommended to review the fuel gas flow to prevent localized high impact on the steel tubes to prevent further failures. An example can be the use of the damper. Concurrently, a review of the steam flow ratio proportionality inside the tube versus gas flow may provide some useful information.

An onsite study needs to be conducted to determine the source of the copper. Copper is not a usual composition or impurities in fuel oil and thus it may have been from other sources.

In-situ metallographic examination and hardness testing need to be carried out on a representative number of remaining superheater tubes, including nearby locations to assess the condition of the remaining tubes. Additionally, periodic *in-situ* metallography and hardness testing should be conducted to assess tubes' condition, especially given evidence of spheroidization, which can accelerate creep and reduce strength faster than expected.

The challenging environmental temperature affected the steel material, as evidenced by minor degradation observed at the inlet elbow which was away from the failed zone. The strength and microstructure were still adequate for continual use at this time. Finally, for better high temperature resistance, chromium nickel or chromium molybdenum steels should be considered.

Conflicts of Interest

The author declares no conflicts of interest regarding the publication of this paper.

References

[1] Jones, D.R.H. (2004) Creep Failures of Overheated Boiler, Superheater and Reformer Tubes. *Engineering Failure Analysis*, **11**, 873-893. https://doi.org/10.1016/j.engfailanal.2004.03.001

[2] Ahmad, J., Purbolaksono, J. and Beng, L.C. (2010) Thermal Fatigue and Corrosion Fatigue in Heat Recovery Area Wall Side Tubes. *Engineering Failure Analysis*, **17**, 334-343. https://doi.org/10.1016/j.engfailanal.2009.06.014

[3] Basu, P., Kefa, C. and Jestin, L. (2000) Erosion Prevention in Boilers. In: Basu, P., Kefa, C. and Jestin, L., Eds., *Boilers and Burners*, Springer, 426-456. https://doi.org/10.1007/978-1-4612-1250-8_15

[4] Stringer, J. (1993) High Temperature Corrosion in Practical Systems. *Le Journal de Physique IV*, **3**, C9-43-C9-61. https://doi.org/10.1051/jp4:1993903

[5] ASTM International (2004) Annual Book of ASTM Standards: (E-3) Standard Guide for Preparation of Metallographic Specimens.

[6] ASTM International (2004) Annual Book of ASTM Standards: (E-407) Practice for Micro Etching Metals and Alloys.

[7] ASTM International (2017) Annual Book of ASTM Standards: (E-384) Standard Test Method for Knoop and Vickers Hardness of Material.

[8] International Organization for Standardization (2013) ISO 18265: 2013, Metallic Materials—Conversion of Hardness Values.

[9] González-Velázquez, J.L. (2018) Elements of Fractography. In: González-Velázquez, J.L., Ed., *Fractography and Failure Analysis*, Springer International Publishing, 21-47. https://doi.org/10.1007/978-3-319-76651-5_2

[10] American Petroleum Institute (2011) API RP 571, Softening (Spheroidization) in Damage Mechanisms Affecting Fixed Equipment in the Refining Industry.

[11] German Institute for Standardization (1979) DIN 17175, Seamless Tubes of Heat Resistance Steel.

[12] American Society for Metals (1988) ASM Metals Handbook: Failures of Boilers and Related Equipment in Failure Analysis and Prevention. 9th Edition, ASM Publications.

[13] American Society for Metals (1987) ASM Metals Handbook: Environmentally Induced Cracking in Corrosion. 9th Edition, ASM Publications.

[14] American Petroleum Institute (2011) API RP 571, Creep and Stress Rupture in Damage Mechanisms Affecting Fixed Equipment in the Refining Industry.

[15] Dillion, J.J., Desch, P.B. and Lai, T.S. (2011) Overheating in the Nalco Guide to Boiler Failure Analysis. 2nd Edition, The McGraw Hill Companies, 61-79.